KANNAN, S., BHOWMICK, P. and ALAMDARI, S.A.S. 2022. Model predictive control of connected spacecraft formation. *IFAC papers online* [online], 55(22): proceedings of the 22nd IFAC (International Federation of Automatic Control) symposium on Automatic control in aerospace 2022 (ACA 2022), 21-25 November 2022, Mumbai, India, pages 322-327. Available from: https://doi.org/10.1016/j.ifacol.2023.03.054

Model predictive control of connected spacecraft formation.

KANNAN, S., BHOWMICK, P. and ALAMDARI, S.A.S.

2022

Available online at www.sciencedirect.com

ScienceDirect

IFAC PapersOnLine 55-22 (2022) 322–327

Model Predictive Control of Connected Spacecraft Formation ⋆

Somasundar Kannan * **Parijat Bhowmick** ** **Seyed Amin Sajadi Alamdari** ***

* *School of Engineering, Robert Gordon University, Aberdeen, AB10 7GJ, UK (e-mail:s.kannan1@rgu.ac.uk)*
** *Dept of EEE, IIT Guwahati, Assam-781039, India (e-mail: parijat.bhowmick@iitg.ac.in)*
*** *Goodyear Operations, Av. Gordon Smith, 7750 Colmar-Berg, Luxembourg*

Abstract: In this contribution we discuss the application of Model Predictive Control (MPC) to achieve a connected network formation of spacecrafts. A set of three spacecrafts are used to achieve in-plane formation which are initially in a connected network. Two scenarios including formation control and formation control with collision avoidance in a leader-follower configuration is addressed through simulation studies. The aspect of MPC stability and network connectivity is also addressed briefly in the context of formation control.

Keywords: Formation Control, Spacecraft, MPC, collision avoidance, connected network.

1. INTRODUCTION

The problem of Spacecraft Formation Flying involves the cooperation of multiple spacecrafts to achieve a common task. The satellite formation can have different mission applications such as [Valmorbida (2014), EO (2016)]: Synthetic Aperture Radar (SAR) mission for remote sensing, Space and Earth Science Missions for acquiring scientific data from multiple satellite locations, Interferometric mission to name a few. There are also different projects that involved formation flying and coordinated control such as [Valmorbida (2014), [EO (2016)]: TanDEM, PRISMA, GRACE, PROBA and LISA among others. Different aspects of the Formation Flying problem has been addressed in literature such as Formation Control and Topology Control. The Formation control [Nair and Behera (2016)] of spacecraft involves the emphasis on the control aspects to obtain relative motion of spacecraft to a certain predefined fixed topology, where as topology control involves the problem of obtaining a certain network topology with specific properties such as connectivity [Moshtagh et al. (2010)]. For an extensive survey on formation control of small satellites please refer to [Liu and Zhang (2018)].

The Model Predictive Control technique has been extensively used for formation and cooperative control [Lavaei et al. (2007); Valmorbida (2014); Scharnagl et al. (2018); Boggio et al. (2022); Kannan et al. (2017); Dentler et al. (2019a,b); Dentler (2018)] due to its advantages of handling constraints systematically including methodologies involving centralized and decentralized solutions.

Compared to [Boggio et al. (2022)] and the references cited in [Liu and Zhang (2018)], the key contributions of this article includes the application of Model Predictive Control to achieve a predefined connected network formation and additionally the problem of stability for a modified problem along with connectivity maintenance in the context of spacecraft formation. The remainder of the article is as follows: first the modelling aspect of the satellite formation flying is addressed using the Clohessy-Wiltshire equation following which the Model Predictive Control is addressed. Next the MPC stability and connectivity is discussed followed by simulation studies.

2. MODELLING

The Clohessy-Wiltshire-Hill [Sidi (1997)] equation which are used for the formation control problem are briefly discussed here starting with the definition of the Hill's frame which can be seen in Fig. 1. Here $\boldsymbol{R}_0$ and $\boldsymbol{R}_1$ are distances of the reference satellite and second satellite from the central body or Earth. The relative distance between the satellites is given by $\boldsymbol{R}_{01} = \boldsymbol{R}_1 - \boldsymbol{R}_0$. For small values of $|\boldsymbol{R}_{01}|$, the relative acceleration in the rotating frame can be given by [Sidi (1997)]

$$\ddot{\boldsymbol{R}}_{01} = \frac{\mu}{R_0^3}\left[-\boldsymbol{R}_{01} + 3\left(\frac{\boldsymbol{R}_0}{R_0}\cdot\boldsymbol{R}_{01}\right)\frac{\boldsymbol{R}_0}{R_0}\right] + \boldsymbol{F} + O(R^2) \quad (1)$$

where $R_0 = |\boldsymbol{R}_0|$, μ is a gravitational constant, $\boldsymbol{F}$ is the external force vector. Under the assumption of circular orbit, the linearized Clohessey-Wiltshire equation can be used to represent the relative motion of follower satellites with respect to a virtual centre [Dai et al. (2013)]

$$\ddot{x}_i - 2n_0\dot{y}_i - 3n_0^2 x_i = u_{x_i} \quad (2)$$

$$\ddot{y}_i + 2n_0\dot{x}_i = u_{y_i} \quad (3)$$

$$\ddot{z}_i + n_0^2\dot{z}_i = u_{z_i} \quad (4)$$

where $[x_i, y_i, z_i]^\top$ are the relative motion states for agent i, $[u_{x_i}, u_{y_i}, u_{z_i}]^\top$ are the control accelerations, $i \in$

⋆ The second author gratefully acknowledges the financial support of the Science and Engineering Research Board (SERB), DST, India, under the research grant SRG/2022/000892/ES.

10.1016/j.ifacol.2023.03.054

$\{1, 2, \ldots, n\}$, $n_0 = \sqrt{(\mu/a_0^3)}$ is the angular velocity of the reference orbit, μ is the gravitational constant of earth and a_0 is the radius of the reference orbit. The above CW equations can be represented as a state-space form $\dot{x}_i = Ax_i + Bu_i$, where A and B can be given by

$$A = \begin{bmatrix} 0 & 0 & 0 & 1 & 0 & 0 \\ 0 & 0 & 0 & 0 & 1 & 0 \\ 0 & 0 & 0 & 0 & 0 & 1 \\ 3n_0^2 & 0 & 0 & 0 & 2n_0 & 0 \\ 0 & 0 & 0 & -2n_0 & 0 & 0 \\ 0 & 0 & -n_0^2 & 0 & 0 & 0 \end{bmatrix} \text{ and } B = \begin{bmatrix} 0 & 0 & 0 & 1 & 0 & 0 \\ 0 & 0 & 0 & 0 & 1 & 0 \\ 0 & 0 & 0 & 0 & 0 & 1 \end{bmatrix}^\top . \tag{5}$$

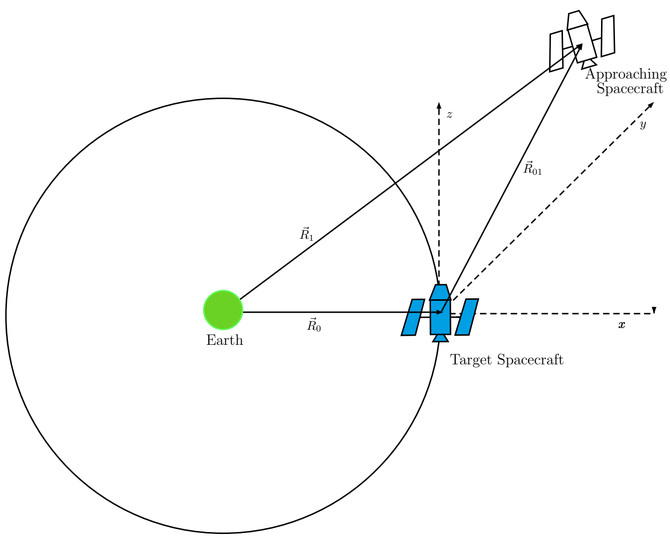

Fig. 1. Hill's Frame.

3. MODEL PREDICTIVE CONTROL (MPC)

The considered plant dynamics within this work can be modelled by the following differential equation

$$\dot{\boldsymbol{x}}(t) = \boldsymbol{f}(\boldsymbol{x}(t), \boldsymbol{u}(t), \boldsymbol{p}(t)) \in \mathbb{R}^n \tag{6}$$

where

$\boldsymbol{x}(t) \in X \subset \mathbb{R}^n$ is the state vector,
$\boldsymbol{u}(t) \in U \subset \mathbb{R}^{m_u}$ is the input vector
$\boldsymbol{p}(t) \in \mathbb{R}^{m_p}$ is the vector of time-dependent parameters.

For means of simplicity, the continuous time formulation will be be first introduced. Based on such a prediction model, a model predictive control (MPC) predicts the plant behaviour for a horizon $\tau = [t, t+T]$ at each time t . Regarding the prediction, the control inputs are determined to minimize a performance index J subject to constraints $\boldsymbol{C} \in \mathbb{R}^{m_c}$. This performance index is generally considered as a cost function. It typically consists of stage costs ℓ which are integrated over the horizon time and final costs φ which express the remaining costs at the end of the prediction horizon. The optimal control problem which has to be solved at each time t is further defined as:

$$\min_{\mathbf{u}} \quad J = \varphi(\boldsymbol{x}_\tau(T,t), \boldsymbol{p}(T,t)) + \int_t^{t+T} \ell(\boldsymbol{x}_\tau(\tau,t), \boldsymbol{u}_\tau(\tau,t), \boldsymbol{p}(\tau,t)) d\tau \tag{7}$$

$$\text{s.t.} \quad \dot{\boldsymbol{x}}_\tau(\tau,t) = \boldsymbol{f}(\boldsymbol{x}_\tau(\tau,t), \boldsymbol{u}_\tau(\tau,t), \boldsymbol{p}(\tau,t)), \tag{8}$$

$$\boldsymbol{x}_\tau(0,t) = \boldsymbol{x}(t), \tag{9}$$

$$\mathbf{0} \geq \boldsymbol{C}(\boldsymbol{x}_\tau(\tau,t), \boldsymbol{u}_\tau(\tau,t), \boldsymbol{p}(\tau,t)). \tag{10}$$

The predicted trajectories $\boldsymbol{x}_\tau$,$\boldsymbol{u}_\tau$ within the horizon are indexed by τ. The feedback of the controller is introduced by (9), as the actual state $x(t)$ is used as initial state $\boldsymbol{x}_\tau(0,t)$ for the optimal control problem.

Practically a discrete-time version of model predictive control is employed and hence we have discrete-time model of the plant sampled at $T > 0$ given as

$$\boldsymbol{x}(k+1) = f_T(\boldsymbol{x}, \boldsymbol{u}). \tag{11}$$

The corresponding cost function $J_N : X \times U^N \to \mathbb{R}_{\geq 0}$ for our problem is defined as

$$J_N(\boldsymbol{x}_0, \boldsymbol{u}) := \sum_{n=0}^{N-1} \ell(\boldsymbol{x}_{\boldsymbol{u}}(n), \boldsymbol{u}(n)) \tag{12}$$

and the respective optimal value function $V_N : X \to \mathbb{R}_{\geq 0} \cup \{\infty\}$ is defined as

$$V_N(\boldsymbol{x}_0) := \inf_{\boldsymbol{u} \in \mathscr{U}^N(\boldsymbol{x}_0)} J_N(\boldsymbol{x}_0, \boldsymbol{u}) \tag{13}$$

for $N \in \mathbb{N} \cup \{\infty\}$. Recursive feasibility of the MPC is ensured by allowing $\boldsymbol{u} = \mathbf{0}$ for arbitrary $\boldsymbol{x}(k) \in X$ that is $\mathscr{U}^N(f_T(\boldsymbol{x}, \boldsymbol{u}_N(\boldsymbol{x}))) \neq \emptyset$. More details on the feasibility issues have been addressed in [Grüne et al. (2010)] and [Worthmann et al. (2016)]. Although feasibility is ensured in the current implementation, asymptotic stability is not guaranteed because in this paper there are no constraints on terminal and running costs. In the following section we will systematically address the asymptotic stability by finding conditions on the prediction horizon N.

4. STABILITY AND CONNECTEDNESS

In this section we will first present some preliminary results necessary to address the closed loop asymptotic stability of spacecraft and finally connectivity and formation flying.

4.1 Stability of MPC

The following assumption introduced in [Tuna et al. (2006)] and discussed in [Worthmann et al. (2016)] is essential here to address the asymptotic stability.

Assumption 1. (Worthmann et al. (2016)). Let a monotonically increasing and bounded sequence $(\gamma_i)_{i \in \mathbb{N}}$ be given and suppose for each $\boldsymbol{x}_0 \in X$ the estimate

$$V_i(\boldsymbol{x}_0) \leq \gamma_i \cdot \ell^\star(\boldsymbol{x}_0) \quad \forall i \in \mathbb{N} \tag{14}$$

holds, where V_i is an optimal value function and $\ell^\star$ is the respective running cost for the desired state $\boldsymbol{x}^\star$. Further, let there exist two $\mathscr{K}_\infty$-functions $\underline{\eta}, \overline{\eta} : \mathbb{R}_{\geq 0} \to \mathbb{R}_{\geq 0}$ satisfying

$$\underline{\eta}(\|\boldsymbol{x} - \boldsymbol{x}^\star\|) \leq \ell^\star(\boldsymbol{x}) \leq \overline{\eta}(\|\boldsymbol{x} - \boldsymbol{x}^\star\|) \quad \forall \boldsymbol{x} \in X. \tag{15}$$

Based on Assumption 1 and if recursive feasibility of our problem holds then asymptotic stability of our closed loop system can be established. We will follow the approach of [Worthmann et al. (2016)] and for detailed discussion please refer to [Grüne et al. (2010)].

Theorem 2. (Worthmann et al. (2016)). Let Assumption 1 hold and let the performance index α_N be given by

$$\alpha_N := 1 - \frac{(\gamma_N - 1)\prod_{k=2}^{N}(\gamma_k - 1)}{\prod_{k=2}^{N}\gamma_k - \prod_{k=2}^{N}(\gamma_k - 1)}. \quad (16)$$

Then, if $\alpha_N > 0$, the relaxed Lyapunov inequality

$$V_N(\boldsymbol{f}_T(\boldsymbol{x}, \boldsymbol{u}_N(\boldsymbol{x}))) \leq V_N(\boldsymbol{x}) - \alpha_N \ell(\boldsymbol{x}, \boldsymbol{u}_N(\boldsymbol{x})) \quad (17)$$

holds for all $\boldsymbol{x} \in X$ and the closed loop MPC with prediction horizon N is asymptotically stable. Here $\boldsymbol{f}_T(\cdot,\cdot)$ is the discrete equivalent of the given continuous system to be controlled.

The above condition (15) on the quadratic running cost and the growth bound $\gamma_i, i \in \mathbb{N}_0$ of condition (14) can be derived using the following:

Theorem 3. (Worthmann et al. (2016)). Let a sequence $(c_n)_{n\in\mathbb{N}_0} \subseteq \mathbb{R}_{\geq 0}$ be given and assume that $\sum_{n=0}^{\infty} c_n < \infty$ holds. In addition suppose that for each $\boldsymbol{x}_0 \in X$ an admissible sequence of control values $\boldsymbol{u}_{\boldsymbol{x}_0} = (\boldsymbol{z}_0(n))_{n\in\mathbb{N}_0} \in \mathscr{U}^\infty(\boldsymbol{x}_0)$ exists such that the inequality

$$\ell(\boldsymbol{x}_{\boldsymbol{u}_{\boldsymbol{x}_0}}(n; \boldsymbol{x}_0), \boldsymbol{u}_{\boldsymbol{x}_0}(n)) \leq c_n \cdot \ell^\star(\boldsymbol{x}_0) \;\; \forall n \in \mathbb{N}_0 \quad (18)$$

holds. Then, the growth bound $\gamma_i, i \in \mathbb{N}_0$ of condition (14) is given by $\gamma_i = \sum_{n=0}^{i-1} c_n, i \in \mathbb{N}_0$.

4.2 Spacecraft control using MPC and stability discussion

In order to apply the above stability results we will simplify our spacecraft control problem. Considering motion along (x, y)-plane and assuming that the spacecraft moves only along the y-axis , we consider the Clohessey-Wiltshire equation as a second order system

$$\ddot{y} = u \quad (19)$$

where we have omitted the subscripts for ease of notation. A discrete equivalent of the system can be given as follows

$$y(k+1) = \begin{pmatrix} y_1 + Ty_2 + T^2u/2 \\ y_2 + Tu \end{pmatrix} \quad (20)$$

where we have the state vector $y = [y_1 \; y_2]^\top$, T is the sample period and u is the control input. For a constant known T we have the system model

$$y(k+1) = Ay + Bu \quad (21)$$

The desired equilibrium $y^\star$ is contained inside X. The running cost chosen here is $\ell(y, u) = \|y - y^\star\|^2 + \lambda\|u\|^2$, where $\lambda \geq 0$. We define a control

$$u(k) = K(y^\star - y_{u_{y_0}}(k; y_0)). \quad (22)$$

K is a design choice which can be chosen such that $u(k) \in U$ for $y_{u_{y_0}} \in X$. We know that

$$y_{u_{y_0}}(k+1; y_0)) = Ay_{u_{y_0}}(k; y_0)) + BK(y^\star - y_{u_{y_0}}(k; y_0))). \quad (23)$$

Let us take

$$y^\star(k+1) = Ay^\star \quad (24)$$

for which we obtain the following

$$\|y_{u_{y_0}}(k+1; y_0) - y^\star(k+1)\| = (A - BK)\|y_{u_{y_0}}(k; y_0) - y^\star\|. \quad (25)$$

Using the running cost we can deduce the condition (18) as follows

$$\begin{aligned} &\ell(y_{u_{y_0}}(k), u_{y_0}(k)) \\ &= \|y_{u_{y_0}}(k) - y^\star\|^2 + \lambda\|u_{y_0}(k)\|^2 \\ &= (1 + \lambda K^2)\|y_{u_{y_0}}(k) - y^\star\|^2 \\ &= (1 + \lambda K^2)(A - BK)^{2k}\|y_{u_{y_0}}(0) - y^\star\|^2 \\ &= c_n \ell^\star(y_0) \end{aligned}$$

In the above demonstration, we have the condition, (18), with $c_n = C\sigma^n$ where $C = 1 + \lambda K^2$ and $\sigma = (A - BK)^2$. Without precisely calculating coefficients c_n and the series γ_i, we will make the stability arguments similar to [Grüne (2021)]. We can note that $C > 0$ and similarly if we consider that the pair (A, B) is stabilizable for a prudently chosen K we have the eigenvalues of σ in the unit circle and for large N we have c_n bounded and finally γ_i bounded. Following the discussion of [Grüne (2021)] we can say that for γ_i bounded we have $\alpha_N \to 1$ as $N \to \infty$. Therefore $\alpha_N > 0$ for sufficiently large N rendering the system asymptotically stable.

4.3 Connectivity and Formation Flying

Here we will briefly discuss the connectivity problem of the multiple spacecraft problem in the lines of the [Kohler and Dimarogonas (2016)]. Let us consider the dynamics of two agent satellites in single dimension, which can be simplified as a double integrator system. More precisely connectedness here is discussed in terms of continuous agent satellite model as it is associated with the original Clohessey-Wiltshire equation. Let us define the relative agent states $\varepsilon := [x_{ij}, v_{ij}]^\top$ with $x_{ij} := x_i - x_j$ and $v_{ij} := v_i - v_j$. Two agents in a proximity-based network which are initially connected will stay connected if their relative states remain in $\Phi = \{(x_{ij}, v_{ij}) | \; \|x_{ij}\| \leq \delta\}$ which is invariant under [Kohler and Dimarogonas (2016)]

$$\dot{x}_{ij} = v_{ij} \quad (26)$$

$$\dot{v}_{ij} = u_i - u_j \quad (27)$$

The one-dimensional relative agent dynamics can be given by [Kohler and Dimarogonas (2016)]

$$\dot{\varepsilon} = \begin{pmatrix} \dot{x}_{ij} \\ \dot{v}_{ij} \end{pmatrix} = A\varepsilon_{ij} + \bar{\mu}_{ij} \quad (28)$$

where $\bar{\mu}_{ij} = \begin{pmatrix} 0 \\ \mu_{ij} \end{pmatrix}$ and considered as a disturbance. Considering the fact that A is Hurwitz, the Lyapunov equation $A^\top P + PA = -Q$ with Q positive definite we have the following Lyapunov function for the system $V_{ij} = \varepsilon_{ij}^\top P \varepsilon_{ij}$ with $P = \begin{bmatrix} P_1 & P_2 \\ P_2 & P_3 \end{bmatrix}$ is symmetric and positive definite. The derivative of the Lyapunov function along the system trajectory gives [Kohler and Dimarogonas (2016)]

$$\dot{V}_{ij} = -\varepsilon_{ij}^\top Q \varepsilon_{ij} + 2\varepsilon_{ij}^\top P \bar{\mu}_{ij} \quad (29)$$

$$\leq 0 \text{ for } \|\varepsilon_{ij}\| \geq 2\|\mu_{ij}\| \frac{\sqrt{P_2^2 + P_3^2}}{\lambda_{min}(Q)} \quad (30)$$

From the above, we get [Kohler and Dimarogonas (2016)]

$$\|\mu_{ij}\| \leq \frac{\lambda_{min}(Q)}{2\sqrt{P_2^2 + P_3^2}}\|\varepsilon_{ij}\| \quad (31)$$

Choosing c^* such that [Kohler and Dimarogonas (2016)]

$$\max_{\varepsilon_{ij}^\top P \varepsilon_{ij} = c^*} \|x_{ij}\| \leq \delta \quad (32)$$

which gives us $c^* = \left(P_1 - \frac{P_2^2}{P_3}\right)\delta^2$ and the following set $\Phi_{c^*} = \{\varepsilon_{ij} | \varepsilon_{ij}^\top P \varepsilon_{ij} \leq c^*\}$.

Theorem 4. (Kohler and Dimarogonas (2016)). The two agen whose dynamics is given by (28) will stay connected at all times if their initial conditions are chosen from the set $\Phi_{c^*} = \{\varepsilon_{ij} | \varepsilon_{ij}^\top P \varepsilon_{ij} \leq c^*\}$ with P being the unique solution of the Lyapunov function for any positive definite Q, c^* such that (32) holds and $\|\mu\|$ is bounded by (31).

Theorem 4 along with the discussions given in the previous section can be used to conclude that the proposed MPC solution will keep the multiple spacecrafts connected while assuring closed loop asymptotic stability. In the following section, we will address a few application scenarios for the cooperative control of spacecrafts.

5. SIMULATION STUDIES

Here we will discuss the application of Model Predictive Control to the problem of Spacecraft Formation Flying. The solution of optimal control problem (8)–(10) is computationally expensive. Furthermore control applications require real-time capability. Therefore model predictive control in space applications is particularly challenging due to limited computational power. For this reason a fast continuation generalized minimal residual method (CGMRES) [Ohtsuka (2004)] is applied within this work. Its computational efficiency has been shown for single plants in [Sajadi-Alamdari et al. (2016)], [Dentler et al. (2016b)], [Seguchi and Ohtsuka (2002)] and [Seguchi and Ohtsuka (2003)], as well its applicability for multi agent systems has been discussed in [Dentler et al. (2016a)]. A major advantage is also the open source code which is available under [Ohtsuka (2015)].

For simulation case study, we have considered a set of three identical spacecrafts. The governing equations are based on the Clohessy-Wiltshire (CW) equation as discussed before with $n_0 = 0.0011$. Two simulation scenarios for in-plane formation are discussed which include: Position Control to achieve connected Network and finally position control with collision avoidance in leader-follower configuration.

5.1 Position Control to achieve a predefined Connected Network Formation

The first scenario includes the formation control of a set of 3 satellites to achieve a predefined connected network formation in-plane. The 3 satellites start from condition $[x_i, y_i, z_i] = [0, 0, 0]$ for $i = \{1, 2, 3\}$ to the final position $[x_1, y_1, z_1] = [100, 100, 100]$, $[x_2, y_2, z_2] = [100, 200, 100]$, $[x_3, y_3, z_3] = [100, 300, 100]$. It is assumed that the in-plane formation already forms a connected network. The cost function used to perform the given control problem can be given as:

$$J_1 = e_p^\top Q e_p + u^\top R u \quad (33)$$

where e_p is the respective position error, $-50 \leq u \leq 50$ is the control input, while Q, R are respectively position and control gains.

The respective simulation results for the current scenario can be seen in Fig. 2,3,4. In Fig. 2 we can see the position evolution of Spacecraft-1 from $[0, 0, 0]$ to $[100, 100, 100]$ with respectively the velocities and control input. In Fig. 3 and Fig. 4, we can respectively see the states and inputs of spacecraft-2 and spacecraft-3.

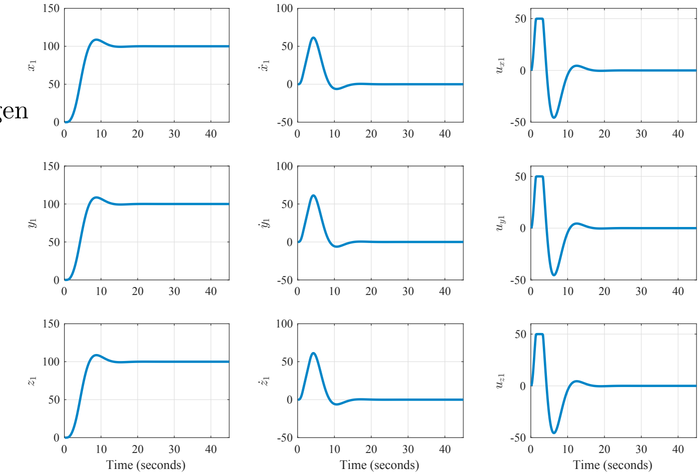

Fig. 2. Position Control: Spacecraft-1.

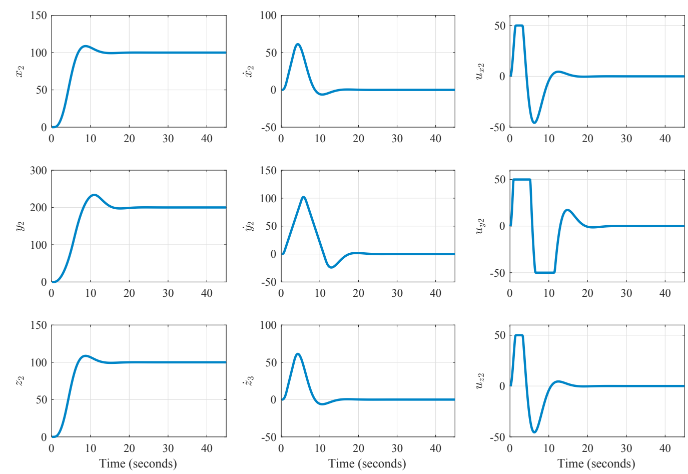

Fig. 3. Position Control: Spacecraft-2.

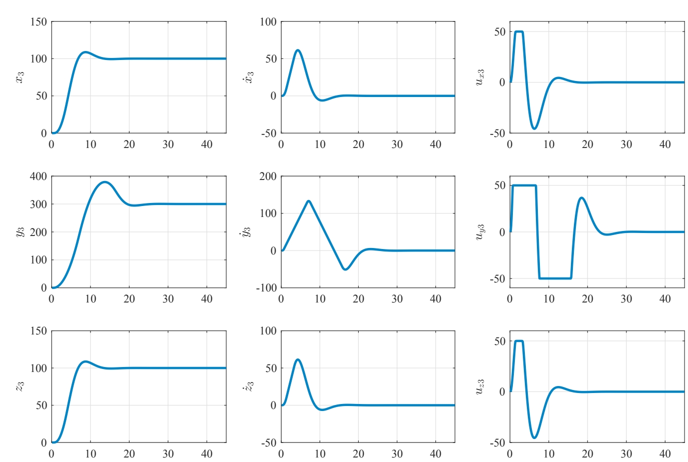

Fig. 4. Position Control: Spacecraft-3.

5.2 Position Control with collision avoidance

The second scenario includes the formation control of a set of 3 satellites to achieve a predefined connected network formation in-plane while following a leader-follower configuration at the same time performing collision avoidance. The 3 satellites start from condition $[x_i, y_i, z_i] = [0, 0, 0]$ for $i = \{1, 2, 3\}$ while only the final position of second satellite is known as $[x_2, y_2, z_2] = [100, 100, 100]$. The first and the third satellite has to reach the final state while maintaining a distance of 10 m from the second satellite. The final x and z positions of the all three satellites are same. It is also assumed that the in-plane formation already forms a connected network. The cost function used to perform the given control problem can be given as:

$$J_1 = e_p^\top Q e_p + u^\top R u + e_{y1}^\top K_1 e_{y1} + e_{y3}^\top K_2 e_{y3} \tag{34}$$

where e_p is the respective position error, $-50 \leq u \leq 50$ is the control input and, $e_{y2} = y_2 - y_1 - 10$ and $e_{y2} = y_2 - y_3 - 10$ are the implicit constraints to maintain the y position of satellite-1 and satellite-3 at 10 m away from satellite-2 with K_1 and K_2 respectively the performance gains. while Q, R are respectively position and control gains.

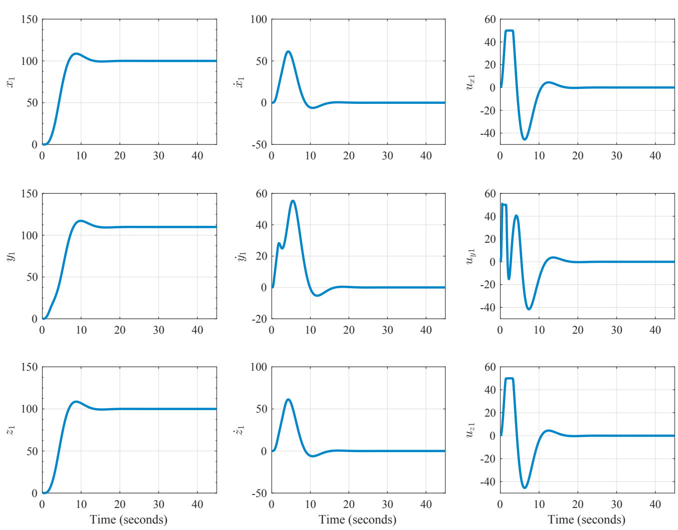

Fig. 5. Position Control with collision avoidance: Spacecraft-1.

The respective simulation results for the current scenario can be seen in Fig. 5,6,7. In Fig. 5 we can see the position evolution of Spacecraft-1 from $[0, 0, 0]$ to $[100, 110, 100]$ with respectively the velocities and control input. In Fig. 6 evolution of Spacecraft-2 from $[0, 0, 0]$ to $[100, 100, 100]$ and in Fig. 4 we can respectively see the states and inputs of spacecraft-3 reaching $[100, 90, 100]$.

6. CONCLUSION

In the current research we have successfully discussed the application of Model Predictive Control to the proximity network formation. The stability of closed loop MPC and connectivity of the spacecraft network is also briefly addressed and two scenarios of simulation including position control and position control with collision avoidance in a leader-follower network is addressed. In the future scope, Negative Imaginary (NI) systems theory [Bhowmick and Lanzon (2022, 2019, 2020); Bhowmick and Patra (2017); Kurawa et al. (2021); Lanzon and Bhowmick (2022); Kurawa et al. (2019); Bhowmick and Ganguly (2022)] can be applied to design a state-of-the-art formation control scheme for a group of connected satellites.

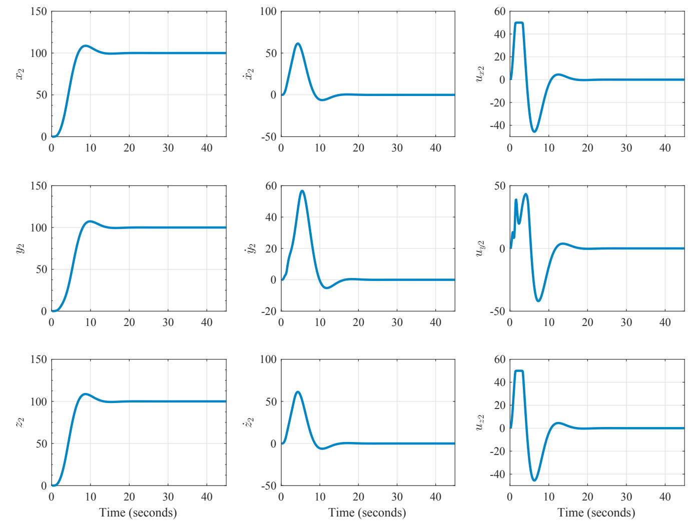

Fig. 6. Position Control with collision avoidance: Spacecraft-2.

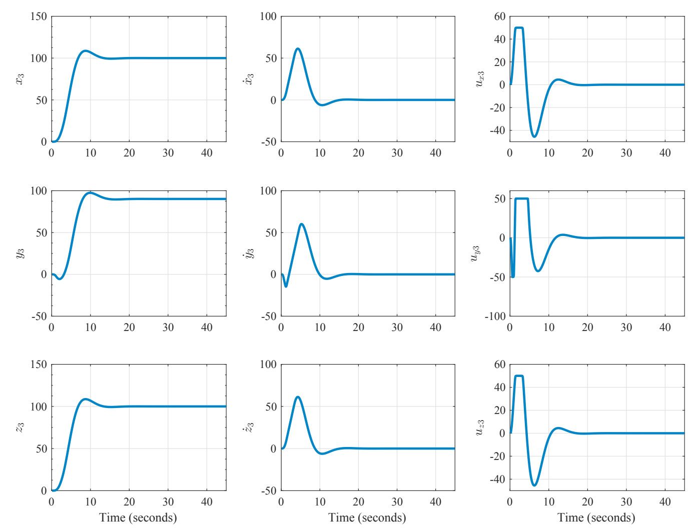

Fig. 7. Position Control with collision avoidance: Spacecraft-3.

REFERENCES

(2016). *Earth Observation Portal*. URL `https://directory.eoportal.org/web/eoportal/home`.

Bhowmick, P. and Ganguly, A. (2022). Vibration control of a class of mechatronic systems using negative imaginary theory. *IFAC-PapersOnLine*, 55(1), 14–19. 7th International Conference on Advances in Control and Optimization of Dynamical Systems ACODS 2022.

Bhowmick, P. and Lanzon, A. (2019). Output strictly negative imaginary systems and its connections to dissipativity theory. In *Proceedings of the 58th IEEE Conference on Decision and Control*, 6754–6759.

Bhowmick, P. and Lanzon, A. (2020). Time-domain output negative imaginary systems and its connection to

dynamic dissipativity. In *Proceedings of the 59th IEEE Conference on Decision and Control*, 5167–5172.
Bhowmick, P. and Lanzon, A. (2022). On discrete-time output negative imaginary systems. *IEEE Control Systems Letters*, 6, 1124–1129.
Bhowmick, P. and Patra, S. (2017). On LTI output strictly negative-imaginary systems. *Systems & Control Letters*, 100, 32–42.
Boggio, M., Colangelo, L., Virdis, M., Pagone, M., and Novara, C. (2022). Earth gravity in-orbit sensing: MPC formation control based on a novel constellation model. *Remote Sensing*, 14(12).
Dai, R., Maximoff, J., and Mesbahi, M. (2013). Optimal trajectory generation for establishing connectivity in proximity networks. *IEEE Transactions on Aerospace and Electronic Systems*, 49(3), 1968–1981.
Dentler, J., Kannan, S., Mendez, M.A.O., and Voos, H. (2016a). A modularization approach for nonlinear model predictive control of distributed fast systems. In *Proceedings of the 24th Mediterranean Conference on Control and Automation*, 292–297.
Dentler, J., Kannan, S., Mendez, M.A.O., and Voos, H. (2016b). A real-time model predictive position control with collision avoidance for commercial low-cost quadrotors. In *Proceedings of the IEEE Multi-Conference on Systems and Control*.
Dentler, J. (2018). *Real-time Model Predictive Control for Aerial Manipulation*. Ph.D. thesis, University of Luxembourg.
Dentler, J., Kannan, S., Bezzaoucha, S., Olivares-Mendez, M.A., and Voos, H. (2019a). Model predictive cooperative localization control of multiple UAVs using potential function sensor constraints. *Autonomous Robots*, 43(1), 153–178.
Dentler, J., Rosalie, M., Danoy, G., Bouvry, P., Kannan, S., Olivares-Mendez, M.A., and Voos, H. (2019b). Collision avoidance effects on the mobility of a UAV swarm using chaotic ant colony with model predictive control. *Journal of Intelligent & Robotic Systems*, 93(1), 227–243.
Grüne, L. (2021). *Nominal Model-Predictive Control*, 1461–1467. Springer International Publishing, Cham.
Grüne, L., Pannek, J., Seehafer, M., and Worthmann, K. (2010). Analysis of unconstrained nonlinear mpc schemes with time varying control horizon. *SIAM Journal on Control and Optimization*, 48(8), 4938–4962.
Kannan, S., Alamdari, S.A.S., Dentler, J., Olivares-Mendez, M.A., and Voos, H. (2017). Model predictive control for cooperative control of space robots. *AIP Conference Proceedings*, 1798(1).
Kohler, P.N. and Dimarogonas, D.V. (2016). On topological conditions to maintain leader-follower connectivity in double-integrator multi-agent systems. In *Proceedings of the 24th Mediterranean Conference on Control and Automation*, 767–772.
Kurawa, S., Bhowmick, P., and Lanzon, A. (2019). Dynamic output feedback controller synthesis using an LMI-based α-strictly negative imaginary framework. In *Proceedings of the 27th Mediterranean Conference on Control and Automation*, 81–86.
Kurawa, S., Bhowmick, P., and Lanzon, A. (2021). Negative imaginary theory for a class of linear time-varying systems. *IEEE Control Systems Letters*, 5(3), 1001–1006.
Lanzon, A. and Bhowmick, P. (2022). Characterisation of input-output negative imaginary systems in a dissipative framework. *in press IEEE Transactions on Automatic Control*, 1–16. DOI:10.1109/TAC.2022.3149938.
Lavaei, J., Momeni, A., and Aghdam, A.G. (2007). A cooperative model predictive control technique for spacecraft formation flying. In *Proceedings of American Control Conference*, 1493–1500.
Liu, G.P. and Zhang, S. (2018). A survey on formation control of small satellites. *Proceedings of the IEEE*, 106(3), 440–457.
Moshtagh, N., Mehra, R., and Mesbahi, M. (2010). Topology control of dynamic networks in the presence of local and global constraints. In *Proceedings of the IEEE International Conference on Robotics and Automation*, 2718–2723.
Nair, R.R. and Behera, L. (2016). Adaptive fuzzy non-singular fast terminal sliding mode control for spacecraft formation flying. In *Proceedingsa of the 1st IEEE International Conference on Control, Measurement and Instrumentation*, 408–413.
Ohtsuka, T. (2004). A continuation/GMRES method for fast computation of nonlinear receding horizon control. *Automatica*, 40(4), 563–574.
Ohtsuka, T. (2015). *Symlab: CGMRES source code*. URL http://www.symlab.sys.i.kyoto-u.ac.jp/~ohtsuka/code/index.htm.
Sajadi-Alamdari, S.A., Voos, H., and Darouach, M. (2016). Nonlinear model predictive extended eco-cruise control for battery electric vehicles. In *Proceedings of the 24th Mediterranean Conference on Control and Automation*, 467–472.
Scharnagl, J., Kremmydas, P., and Schilling, K. (2018). Model predictive control for continuous low thrust satellite formation flying. *IFAC-PapersOnLine*, 51(12), 12–17. IFAC Workshop on Networked and Autonomous Air and Space Systems.
Seguchi, H. and Ohtsuka, T. (2002). Nonlinear receding horizon control of an RC hovercraft. In *Proceedings of the International Conference on Control Applications*, volume 2, 1076–1081.
Seguchi, H. and Ohtsuka, T. (2003). Nonlinear receding horizon control of an underactuated hovercraft. *International Journal of Robust and Nonlinear Control*, 13(3-4), 381–398.
Sidi, M.J. (1997). *Spacecraft Dynamics and Control*. Cambridge University Press.
Tuna, S., Messina, M., and Teel, A. (2006). Shorter horizons for model predictive control. In *Proceedings of the American Control Conference*, 863–868.
Valmorbida, A. (2014). *Development and Testing of Model Predictive Control Strategies for Spacecraft Formation Flying*. Ph.D. thesis, Universita degli Studi di Padova.
Worthmann, K., Mehrez, M.W., Zanon, M., Mann, G.K.I., Gosine, R.G., and Diehl, M. (2016). Model predictive control of nonholonomic mobile robots without stabilizing constraints and costs. *IEEE Transactions on Control Systems Technology*, 24(4), 1394–1406.